



Available online at www.sciencedirect.com

SCIENCE  DIRECT[®]

International Journal of Pharmaceutics 267 (2003) 35–47

international
journal of
pharmaceutics

www.elsevier.com/locate/ijpharm

Atomic force microscopy analysis and confocal Raman microimaging of coated pellets

Ann Ringqvist^a, Lynne S. Taylor^b, Katarina Ekelund^c, Gert Ragnarsson^d,
Sven Engström^e, Anders Axelsson^{a,*}

^a Department of Chemical Engineering, University of Lund, SE-221 00 Lund, Sweden

^b Department of Industrial and Physical Pharmacy, Purdue University, West Lafayette, IN 47907, USA

^c AstraZeneca R&D Lund, SE-221 87 Lund, Sweden

^d AstraZeneca R&D, SE-151 85, Södertälje Sweden

^e Pharmaceutical Technology, Applied Surface Chemistry, Chalmers University of Technology, SE-412 96 Göteborg, Sweden

Received 8 October 2002; received in revised form 22 July 2003; accepted 30 July 2003

Abstract

Polymer-coated pellets with different coating thicknesses have been studied regarding coating morphology and drug release properties with atomic force microscopy (AFM) and confocal Raman microscopy. The results were compared with those from scanning electron microscopy (SEM) and drug release profiles, which have been measured previously for these systems and found to vary depending on coating thickness. Results from AFM studies indicated that these pellets differ in the amount of crystalline material on the surface of the coating. The amount was found to be highest on the pellet with the thinnest coating. Confocal Raman microscopy studies confirmed that the active component (remoxipride hydrochloride monohydrate) is present at or close to the surface and that the amount is higher for the thinnest coating. AFM studies in aqueous media showed that the crystalline material on the surface was almost instantaneously dissolved and released into the liquid. AFM has proven to be a powerful tool in the study of the surface of dry formulations and in the study of the controlled release mechanism of a pharmaceutical in a liquid cell. The method can be combined with Raman, giving the added possibility to identify the chemical composition in selected small areas of the coating surface.

© 2003 Published by Elsevier B.V.

Keywords: Coating; AFM; Controlled release; Confocal Raman microscopy; Pellets; Ethyl cellulose

1. Introduction

Oral controlled release pharmaceuticals are of great importance due to their ability to allow a predetermined controlled release of the drug to obtain favor-

able clinical performance (Sandberg et al., 1988). To accomplish new and better formulations it is necessary to understand the mechanism of controlled drug delivery systems (Wesselingh, 1993). Film coating is a process frequently used to obtain controlled release characteristics, where the active substance is present in the core of the coated tablet or the pellet. The mass transfer of active substance through the coating in this type of formulation is in general the rate-controlling step (Langer, 1993). The coating

* Corresponding author. Tel.: +46-46-222-82-87;
fax: +46-46-222-45-26.

E-mail address: Anders.Axelsson@chemeng.lth.se
(A. Axelsson).

material is usually a polymer, or a polymer mixture, blended with softening and coloring-agents, together with agents required for optimization of the coating process.

The performance of the controlled release preparation i.e. bioavailability and efficiency is dependent on the quality of the coating (Shakesheff et al., 1996). The development of new pharmaceutical formulations with controlled release behavior is today still very much of empirical nature. To increase the understanding of the release behavior, new and more efficient methods for the characterization of coatings are therefore desirable.

Atomic force microscopy (AFM) offers a non-destructive method of characterizing non-conducting surfaces in air and liquid (Bottomley, 1998). AFM, a descendent of scanning tunneling microscopy (STM), belongs to the category of scanning probe microscopy (SPM). Since the invention of AFM the use and range of applications of the method have increased rapidly. The range of applications extends from studies of well-structured inorganic materials on the atomic scale, to living cells in an aqueous environment (Bottomley, 1998). Several *in situ* studies of the degradation of polymers or polymer-containing formulations have been carried out using AFM (Chen et al., 1995; Shakesheff et al., 1995a,b 1994a,b). In the interpretation of the images obtained with AFM, it is essential to consider artifacts created by a number of physical phenomena.

Raman microscopy can be used to produce chemical images of solid dosage forms (Clarke et al., 2001). The sample is placed on a motorized XYZ mapping stage and, using a tightly focused laser beam, Raman spectra are obtained at different points in the sample. By using the appropriate experimental conditions, both spatial and depth resolution can be limited (1–2 μm , best case situation) (Sammon et al., 1999). The aim of the Raman microimaging experiments with the coated pellets was to limit the depth of penetration of the laser into the sample, so that the chemical composition of the coating could be investigated.

In this study three types of coated pellets, which differ in the amounts of ethyl cellulose-based coating, were studied both in air and in liquid using AFM and in air using confocal Raman microscopy. The aim was to obtain better insight into the physical processes taking place during the release of the active substance.

The pellets, containing remoxipride hydrochloride monohydrate (Roxiam[®]) as the active substance, were produced by spray-coating in a Würster-coater. The active component is highly water soluble and an extended release system consisting of a multi-unit membrane coated reservoir formulation had been found to be suitable in order to control drug release rate. The results of the AFM and the confocal Raman microimaging measurements are compared with results from dissolution tests (Borgqvist et al., 2002) and scanning electron microscopy (SEM) studies. SEM offers an alternative, well-established, method for the characterization of surfaces but can not be used for non-invasive studies of coated pellets during the release process in liquids. Furthermore, the potential of AFM and its ability to analyse surface properties of coated controlled release formulations in dry as well as in liquid conditions is exploited in the present study.

2. Materials and methods

2.1. Material

The pharmaceutical pellets used in this study, Roxiam[®], were obtained from AstraZeneca Tablet Production Sweden. The properties and the effects of coating thicknesses were studied. Thicknesses of approximately 8, 13, and 18 μm were obtained by applying 40, 70, and 90 mg coating per gram pellets and the samples are denoted p40, p70, and p90, respectively.

2.2. The formulation of the material

The uncoated pellets, which are 1 mm in diameter, consist mainly of the crystalline active substance, remoxipride hydrochloride monohydrate mixed with microcrystalline cellulose (20%). The active substance and microcrystalline cellulose are mixed with water and extruded. The extruded material is spheronized, dried, and sieved prior to the coating process, in order to obtain the desired pellet size. A water-insoluble polymer (ethyl cellulose and the plasticizer triethyl citrate (10%)) is then used to coat the pellets. The polymer and the plasticizer is dissolved in ethanol and sprayed onto the uncoated pellets in a Würster-coater

with a top spray at a temperature of 60 °C (Borgqvist et al., 2002). After sieving and the addition of glidants about 100 pellets are encapsulated in a gelatin capsule.

2.3. AFM measurements

The AFM measurements were performed repeatedly on many different pellets and on several different areas on each pellet. Although variations were seen, the images presented were typical of those most frequently observed. Contact and tapping mode AFM measurements were performed using a commercial Nanoscope® IIIa (Digital Instruments, Santa Barbara, CA, USA). Contact mode experiments were run in air and in water at ambient temperature. A J tube scanner with a 125×125 (x,y) $\times 5$ (z) μm scan range and an E tube scanner with a 10×10 (x,y) $\times 2.5$ (z) μm scan range were used. Microfabricated, square-pyramidal-shaped tips of silicon nitride, with a bending spring constant of 0.58 N m^{-1} (manufacturer specified, Digital Instruments) were used as received. The scan rate was 2 Hz, and the applied force was of the order of 100–200 nN.

AFM measurements were performed on coated pellets without sample preparation and on pellets that had first been immersed in pure water at 37 °C for 50, 100, 150, 200, 300, or 400 min in a dissolution test vessel with rotating basket according to USP (Dissolutesest, Prolabo, Paris, France) and then dried. The release from the pellets was performed in water that was deionized, distilled, and filtered through a Millipore Q purification system (Millipore Corporation, Bedford, MA, USA).

Measurements were taken under perfect sink conditions in liquid obtained by using a watertight cell with a flow of water. In this experiment, the liquid cell consisted of a washer placed on top of a circular magnetic plate. The washer had a thickness of 1.25 mm and a center hole 4 mm in diameter. The water was deionized, distilled, and filtered through a Millipore Q purification system (Millipore Corporation). In liquid-environment measurements, a water flow of $1 \mu\text{l s}^{-1}$ was used (Ismatec SA, IPN 16 Pump, Laboratoriumstechnik, Glattsbrugg, Zurich, Switzerland). The flow was halted during imaging in order to minimize disturbances. An image was collected before addition of liquid to the cell, and then images

were repeatedly collected with different time gaps. The scan rate was 2 Hz, and the applied force was of the order of 100–200 nN. For every attempt to obtain an image the tip was lowered and the compliance set to obtain the best image.

Tapping mode AFM measurements were performed in air with an E tube scanner. Microfabricated, asymmetric-pyramidal-shaped tips of silicon, Pointprobe® sensor type NCH-W, with a bending spring constant of $27\text{--}62 \text{ N m}^{-1}$ and resonance frequency of 282–367 kHz (NANOSENSORS™ GmbH & Co., Wetzlar-Blankenfeld, Germany) were used as received. The scan rate was of the order of 1–2 Hz.

To eliminate imaging artifacts, the scan direction was varied to ensure that the true image was obtained. The images obtained from contact and tapping mode measurements were modified using the standard software commands “flatten” and “plane fit.” The same algorithms were used for all images.

2.4. Confocal Raman measurements

Images of the pellet coating (on intact pellets) were obtained using a LabRam HR800 Raman microscope (J-Y Horiba), equipped with a 780 nm diode laser and an air cooled charge coupled device detector. The confocal hole was set to $200 \mu\text{m}$, the slit was $100 \mu\text{m}$, and a $950 \text{ grooves mm}^{-1}$ grating was used. Using these conditions the depth resolution is of the order of $3 \mu\text{m}$ (using silicon as a reference material), although it should be noted that this is an approximation and the actual depth resolution is dependent on the optical properties of the sample. An area of $50 \mu\text{m} \times 50 \mu\text{m}$ was mapped using a $100\times$ lens (numerical aperture 0.9) and experiments were performed in triplicate using three individual pellets of each coating thickness. The step size in both the x and y direction was $2 \mu\text{m}$, and stepping was achieved using an encoded XYZ motorized stage. Using magnification under visible light, a sample area from the coated pellet surface was chosen so that an area of $50 \mu\text{m} \times 50 \mu\text{m}$ was in focus. Using the Raman signal generated from illumination with the 780 nm laser, the height of the microscope stage was adjusted to ensure that data would be collected from the outer part of the coating. The grating was centered at 1000 cm^{-1} and data over the spectral range $1200\text{--}800 \text{ cm}^{-1}$ was collected using an

acquisition time of 2 s \times 45 s per point. This spectral range enabled differentiation of the components present.

2.5. SEM measurements

Measurements with SEM (ISI-100A, International Scientific Instruments) were performed on p40, p70, and p90 pellets in a high-vacuum environment, at a potential of 15 kV. The samples were pre-treated by sputtering a 20-nm-thick layer of gold onto the sample surface.

3. Results

3.1. Contact mode AFM measurements in air

Contact mode AFM measurements in air revealed a layer of dried coating droplets, of 2–50 μm in diameter, on the surface of the pellets (Fig. 1(i) and (ii)). In some areas the droplets overlay each other. The coating of the pellets also seems to have a wavy surface, which is indicated by the light and dark pattern in the height image (Fig. 1(i) left and (ii) left). Material of crystalline appearance, i.e. small needle-like particles

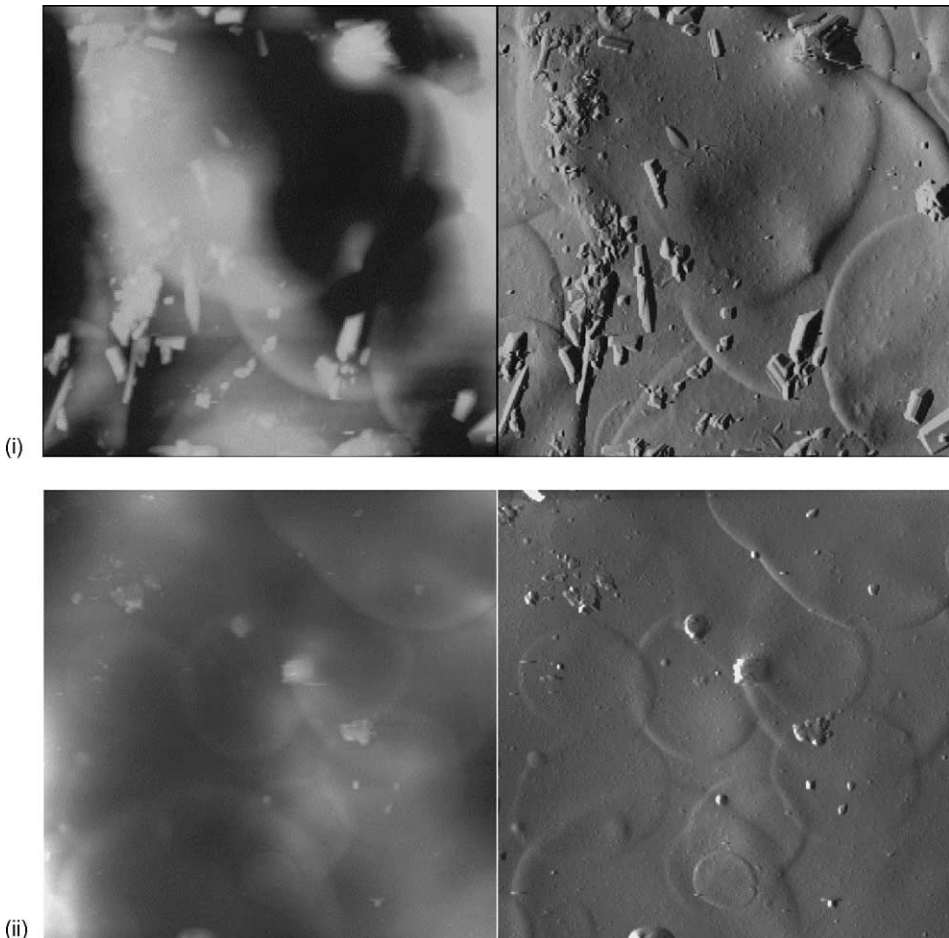


Fig. 1. Height (left) and deflection image (right) from contact mode AFM measurements in air on p40 pellets (i) and p70 pellets (ii), revealing dried spray droplets, a wavy surface, and a difference in amount of material of crystalline appearance between the p40 pellets (i) and the p70 pellets (ii). The height difference between the white and black areas in the height image is 1.6 μm and the size of the surface is (i) 40 $\mu\text{m} \times 40 \mu\text{m}$ and (ii) 50 $\mu\text{m} \times 50 \mu\text{m}$.

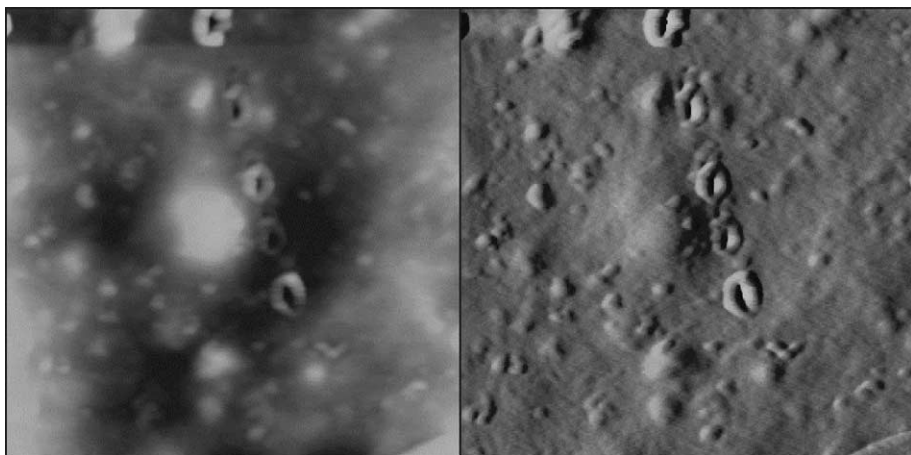


Fig. 2. Small depressions revealed in a height (left) and deflection (right) image from contact mode AFM measurements in air on p40 pellets. In the centre of the image, four large “crater”-like structures of about $0.4\text{ }\mu\text{m}$, larger than most of the depressions, can be observed. The height difference between the white and black areas in the height image is 100 nm and the size of the surface is $4\text{ }\mu\text{m} \times 4\text{ }\mu\text{m}$.

with sharp edges is visible on the exterior of the coating. This material is most frequent on the surface of p40 pellets (Fig. 1(i)). The amount of material of crystalline appearance on p70 (Fig. 1(ii)) and p90 pellets is approximately the same but substantially less than the amount on the p40 pellets. The use of the E tube scanner revealed a more detailed surface structure. Small depressions, 100–200 nm in diameter and 5–25 nm in height, cover the surface of all studied pellets (Fig. 2). Occasionally larger “crater-like” structures of about

$0.4\text{ }\mu\text{m}$ can be seen on some of the pellets. Contact mode AFM measurements in air were also performed on pellets that had been submerged in water for various times and then dried. In these measurements, considerable variations in the polymer coating made it difficult to elucidate the true character of the surface. The only conclusion that could be derived from these measurements was that the crystalline material on the surface had disappeared within 50 min (the shortest measurement time) in water (data not shown).

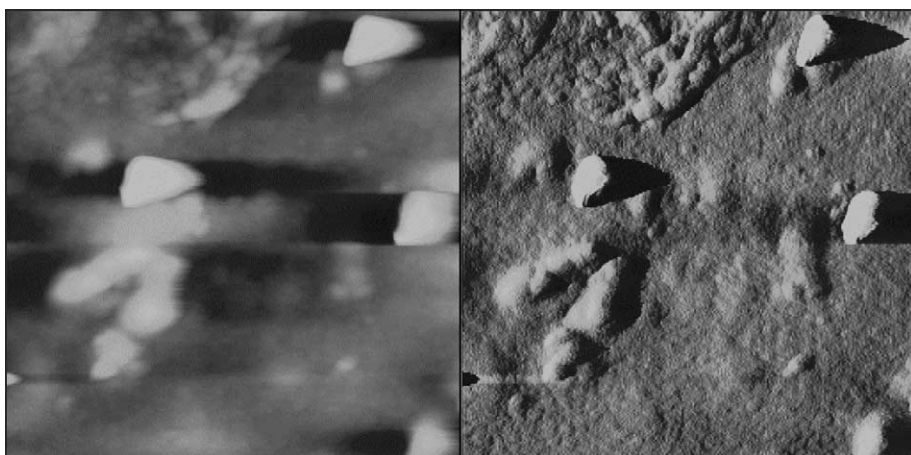


Fig. 3. Polymer surface structure observed at tapping mode AFM measurements in air on p90 pellets. The difference in height between the black and white areas in the right image, the height image, is 50 nm. The left image shows a difference in amplitude. The size of the surface in the image is $1\text{ }\mu\text{m} \times 1\text{ }\mu\text{m}$.

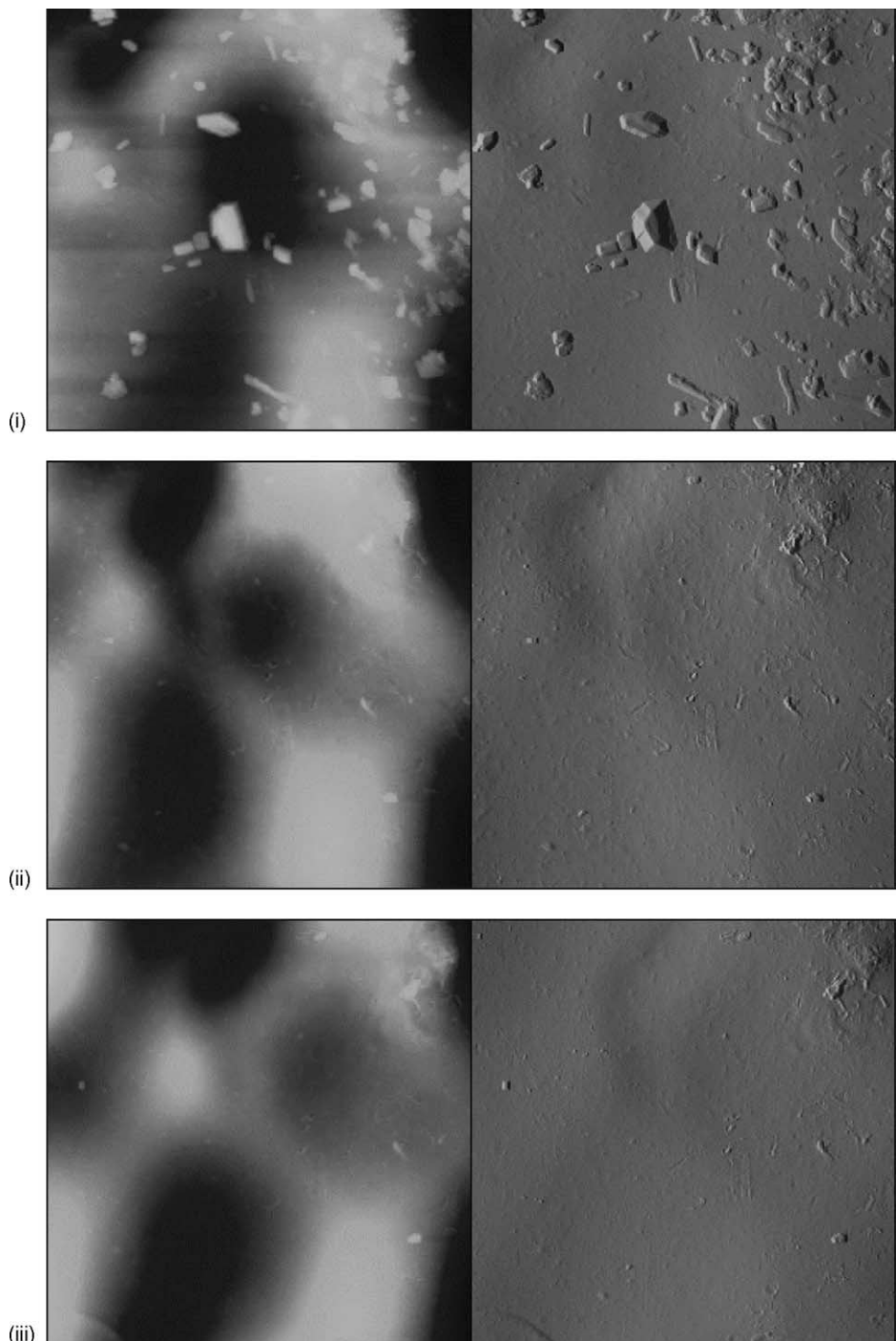


Fig. 4. Height (left) and deflection (right) images from contact mode AFM measurements on p40 pellets in (i) air; (ii) in water after 10 min; and (iii) in water after 30 min. The image series show the change in surface during dissolution. The height difference between the white and black areas in the height images is $1.6 \mu\text{m}$ and the size of the surface is $40 \mu\text{m} \times 40 \mu\text{m}$.

3.2. Tapping mode AFM measurements in air

The results from tapping mode AFM experiments revealed more details of the structure of the coating surface, which could not be detected in contact mode measurements. Fig. 3 shows the same type of small depressions as described earlier (Fig. 2) as well showing that the irregular character of the coating (exterior) consisted of tightly packed depressions, about 30 nm in diameter and 0.8–2.5 nm in height. The “craters” discussed earlier, that occasionally appear in the contact mode studies, do not appear in the tapping mode studies. The apparent “shadows” in Fig. 3 indicating elongated height properties of the raised regions are probably artefacts due to the AFM settings.

3.3. Contact mode AFM measurements in liquid

Fig. 4 shows the behavior of the pellet coating during dissolution in water. The crystalline material on the exterior of the coating dissolves during the first 10 min, as can be seen by comparing Fig. 4(i) and (ii). Other experiments confirmed that the crystals dissolve instantaneously. The conformation of the wavy surface changes during the first 30 min of dissolution, as can be seen in Fig. 4(i)–(iii) (left-hand images), during the swelling of the core and the coating of the pellet.

Between 30 min and 24 h the wavy surface seems to remain unchanged. During contact mode AFM analyses in water with the E tube scanner, which gives a higher resolution than the J tube scanner, difficulties arose in targeting the same area for repeated analysis. Since the difference in surface structure between different areas is significant no conclusions can be derived from these results.

3.4. Confocal Raman measurements

The object of the Raman measurements was to confirm that the crystalline particles observed on the surface of the pellets using the AFM technique were remoxipride HCl monohydrate and to explore in greater detail the chemical composition of the outer part of the coating for the three different pellets. Reference spectra of the coating material (ethyl cellulose) and remoxipride HCl monohydrate were obtained. There is ample spectral contrast between these two substances as can be seen from Figs. 5 and 6. The spectrum of remoxipride HCl monohydrate is characterized by an intense peak at 1000 cm^{-1} whilst the spectrum of ethyl cellulose has broad peaks of which the 875 cm^{-1} peak is most useful for identification since there is no peak in the remoxipride HCl monohydrate spectrum at this position. These peaks were used to build chem-

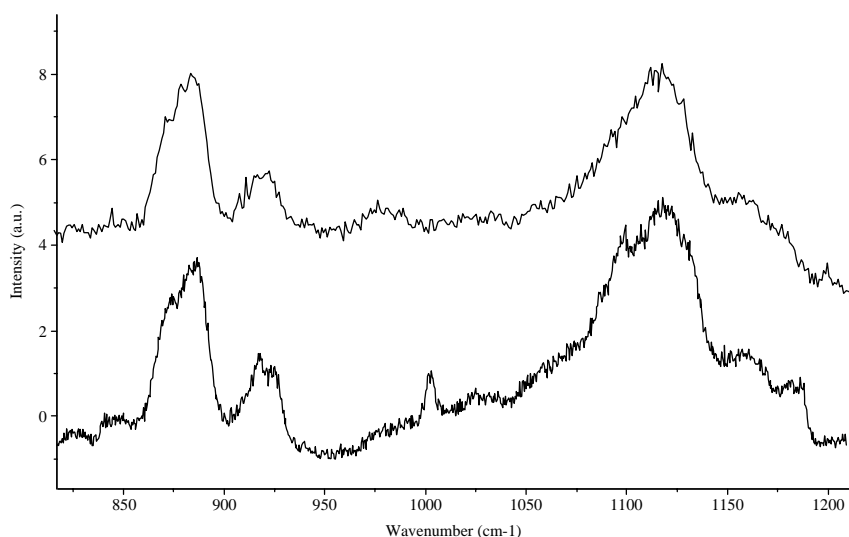


Fig. 5. Top spectrum is reference spectrum of ethyl cellulose; bottom spectrum is extracted from a map obtained from a 40 mg pellet from a region showing a high polymer concentration. Note the weak drug peak at around 1000 cm^{-1} .

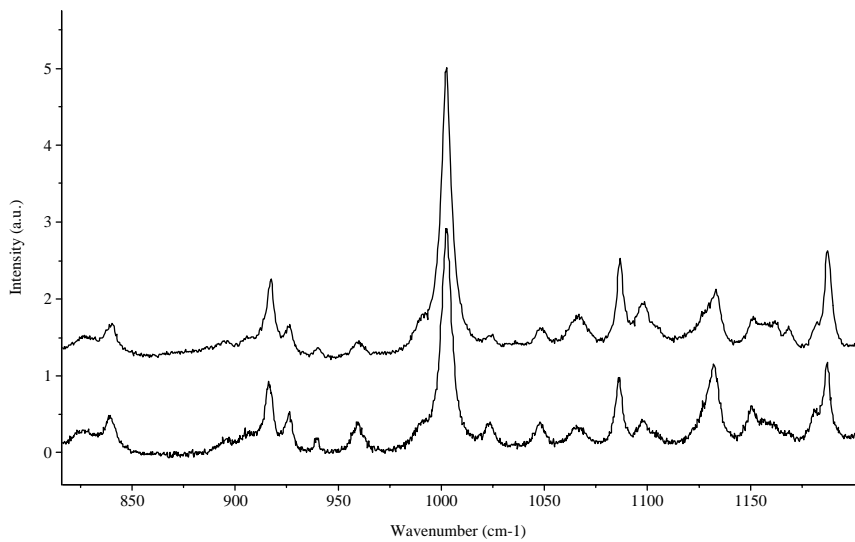


Fig. 6. Top spectrum is pure remoxipride HCl monohydrate; bottom spectrum is extracted from the map of a 40 mg pellet showing a point where there is a high concentration of remoxipride HCl monohydrate.

ical maps to look at the distribution of the drug in the coating. [Fig. 7](#) illustrates such a map, where the white areas show where the spectrum was dominated by remoxipride HCl monohydrate peaks, whereas the dark

areas show ethyl cellulose rich areas. Spectra extracted from the white area and dark regions are shown in [Figs. 5 and 6](#), respectively. A comparison between the spectrum extracted from the remoxipride

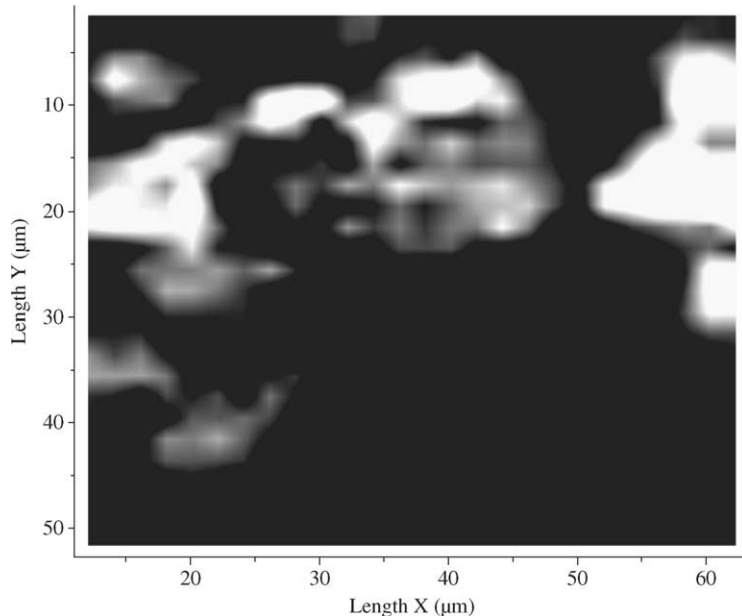


Fig. 7. Chemical image showing the distribution of remoxipride HCl monohydrate in the coating of a 40 mg pellet. The white areas show regions where there is a high concentration of remoxipride HCl monohydrate. The dark areas correspond to ethyl cellulose rich domains.



Fig. 8. Image ($70 \mu\text{m} \times 100 \mu\text{m}$) from SEM measurements on a p40 pellet showing dried spray droplets, a wavy surface and material of crystalline appearance.

HCl monohydrate rich area with that obtained from pure remoxipride HCl monohydrate indicates that the coating contains relatively distinct regions of remoxipride HCl monohydrate which are essentially free of ethyl cellulose. This result indicates that particles of remoxipride HCl monohydrate are present in the coating. The Raman results are consistent with data shown in Figs. 1 and 8, where material of crystalline appearance is seen on the surface of the pellets using AFM and SEM measurements. From the Raman image, it can be seen that the areas rich in remoxipride HCl monohydrate are larger than the crystals seen using the other measurements. However, it should be remembered that both AFM and SEM detect only material present on the surface, while confocal Raman microscopy measures a certain depth into the coating (around $3 \mu\text{m}$ for this system). Hence, any particles present below the surface will also be measured and this most likely accounts for the observed differences in the images obtained with different techniques. For the ethyl cellulose rich regions, an extracted spectrum is very similar to that of the reference ethyl cellulose spectrum with the exception

of the small peak at 1000 cm^{-1} . It was impossible to obtain an ethyl cellulose spectrum from the 40 mg pellet coating which did not contain this peak, which most likely arises from remoxipride HCl monohydrate. This small remoxipride HCl monohydrate peak most likely arises from small particles buried in the coating which are sufficiently close to the surface to contribute to some extent to the Raman signal. For both the 70 and 90 mg pellets, having an estimated coated thickness of 13 and $18 \mu\text{m}$, respectively, remoxipride HCl monohydrate rich areas were not observed. For all the maps obtained the spectra were either pure ethyl cellulose or mainly ethyl cellulose with a small remoxipride HCl monohydrate peak at 1000 cm^{-1} , similar to the spectra shown in Fig. 5 (data not shown).

3.5. SEM measurements

The SEM studies showed that the surface is wavy, that dried droplets in the range of $2\text{--}50 \mu\text{m}$ cover the surface and that small particles are occasionally spread over the surface (Fig. 8).

4. Discussion

Various methods of performing dissolution tests on these pellets have been reported previously (Zackrisson et al., 1995) and a computer program for the simulation and parametric study of data based on these pellets has also been developed (Borgqvist et al., 2002). The dissolution behavior of these pellets is characterized by a short lag period followed by zero order release as shown for p40 pellets in Fig. 9. Similar appearance is obtained for the release from p70 and p90 pellets although the lag time is slightly longer and has a larger variation. Previous studies have shown that the zero order release region can be explained by the mass transfer resistance in the polymer film. Based on that a plausible mechanism for the drug release can be described in the following way. After ingestion of the oral drug, the gelatine capsule is dissolved by the gastric juice. During the lag phase the pellets swell about 3% in 2–8 min due to the penetration of water. The water dissolves part of the active substance instantaneously. The diffusion of the active substance from the pellet begins immediately after the dissolution of

active substance has started in the pellet. During the constant rate release period a saturated solution of the active component is present within the pellet giving a constant driving force for the release (Borgqvist et al., 2002). The release of the drug from pellets is limited by the mass transfer of the drug through the coating layer and is constant as long as some undissolved drug remains in the pellets (Ragnarsson et al., 1992). Dissolution data for single-pellet release experiment on p40 pellets, where the concentration of dissolved substance (kg m^{-3}) is plotted against time (h) in Fig. 9 (Borgqvist et al., 2002). The plotted data shows a great variation in the release profiles for different pellets. It was postulated in that work that a number of processes might contribute to the variation in lag time before the zero order release was reached, beyond the actual thickness of the coating. Results from those studies indicate that the coating composition is more complex than previously thought.

The results from the SEM studies were in good agreement with the results from the AFM studies with both techniques enabling visualization of dried coating droplets, the wavy surface of the coated pellets

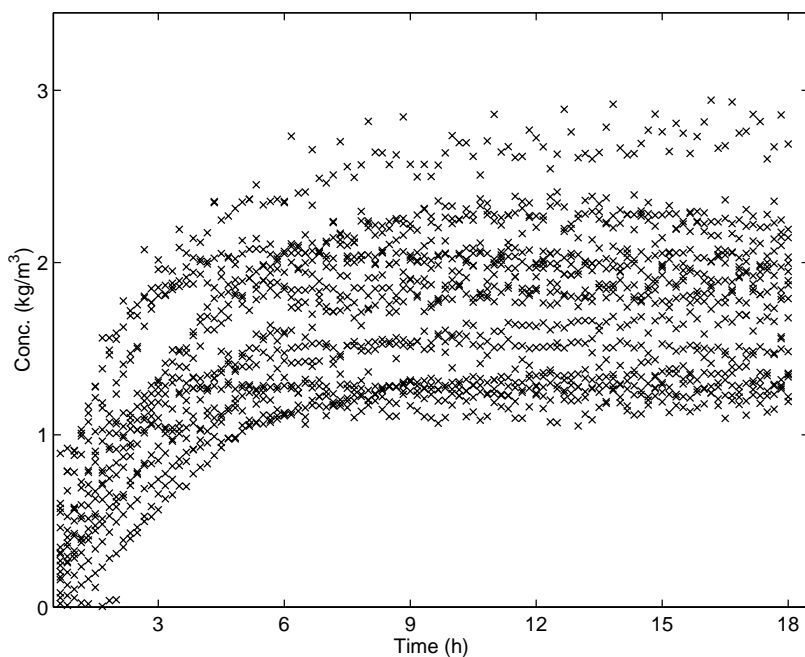


Fig. 9. Dissolution data for single-pellet release experiment on p40 pellets, where the concentration of dissolved substance (kg m^{-3}) is plotted against time (h) (Borgqvist et al., 2002).

and material with a crystalline appearance dispersed over the pellet surface, as is apparent by comparing Figs. 1 and 4(i) with Fig. 8. The wavy surface shown in Figs. 1, 4 and 8 may be due to the underlying texture of the core structure and/or result from particle shrinkage during drying. No cracks in the coating were observed indicating that the coating forms a continuous barrier in the pellets studied. These were selected from the batch manually avoiding pellets that were aggregated. However, the presence of crystalline deposits in the coating, particularly for the 40p pellets suggests that the coating is not homogeneous. The material of crystalline appearance may be fragments of the core that arose during the coating process during production. The pellets are sieved before the coating process to eliminate or reduce the amount of fine particles normally present in a batch of pellets. However some small particles may remain and other small particles may be formed by attrition of the pellets during the initial stage of the coating process, before the coating layer has been established. It is also possible that individual pellets with inferior mechanical properties fragment, produce fine particles. These processes may contribute to a larger amount of fine particles of core material, during the early stage of the coating process compared with later stages. Consequently, we should expect a higher amount of crystalline material on the pellets with the thinnest coating. A continuous attrition of material during the initial coating step would also mean that crystalline material would be embedded in the coating. During dissolution embedded crystals may form cavities and pores in the coating, which may create a percolation network. A porous structure will increase the drug release rate, which may explain the higher release rate from the pellets compared to that predicted from the drug diffusion rate through a pure ethyl cellulose coating. However, the AFM studies using the liquid cell and the J tube scanner did not show any example of this due to the limit in resolution. The E scanner is not suitable for AFM measurements in liquid for this application due to the considerable variation in the surface structure of the material used. However, a more precise navigation controller may solve this problem. This would facilitate repeated scanning of a given surface area thus providing further insight into the release mechanism. The rapid onset of drug release and lack of lag time (Fig. 9) (Borgqvist

et al., 2002) in some of the pellets release profiles are probably due to rapid dissolution of the active agent present on, and embedded in, the coating layer. The small depressions visualized in Fig. 2 could indicate the presence of embedded particles in the coating created in the coating process. These particles most probably emanate from broken remoxipride needle-like crystals. The crater-like structure could be the starting point for a percolation network explaining the absence of a lag phase in the release profile for some of the pellets (Fig. 9). The embedded material is made up of small pieces of the needle-like crystals of the active substance. The surface roughness that the tapping mode measurements indicated (Fig. 3) may have several origins. The structure may arise from irregularities during the drying of the coating. During the contact mode AFM measurements in water was concluded that the crystalline material dissolves or is discharging instantaneously from the surface, comparing Fig. 4(i) and (ii). This may explain the lack of a lag phase and the burst-release phenomena in some of the release profiles in Fig. 9. The apparent swelling of the pellets when immersed in water, noted in the contact mode measurements in water, may be due to passive uptake of water, but may also be caused by hydrostatic pressure due to osmotic forces acting over the polymer coating (Lindstedt et al., 1989). Such an effect indicates that the porosity is not becoming large enough to eliminate the hydrostatic pressure caused by the osmotic pressure difference across the coating layer.

In the confocal Raman microscopy measurements it was shown that it was impossible to obtain a pure ethyl cellulose spectrum from the 40 mg pellet coating. The existence of the peak at 1000 cm^{-1} which most likely arises from remoxipride HCl monohydrate, suggests that either the laser is penetrating through the coating and picking up some remoxipride HCl monohydrate in the core (which is unlikely since the analysis was conducted in confocal mode and the coating is estimated to be $8\text{ }\mu\text{m}$, greater than the estimated depth resolution), or that there is a trace amount of remoxipride HCl monohydrate in all parts of the coating. The results from the confocal Raman measurements of the p70 and the p90 pellets indicate that there are few remoxipride HCl monohydrate drug particles close to the outer surface of the coating and that the coating is much more homogeneous in these pellets than in the 40 mg pellets. Thus, Raman microspectroscopy con-

sequently confirmed that remoxipride HCl monohydrate is present in the coating of the 40 mg pellets. This is in agreement with the interpretation of the AFM data. The presence of remoxipride HCl monohydrate on the surface of the pellet coating for the 40 mg pellets is consistent with the hypothesis that drug particles/dust become embedded in the coating during the coating process due to attrition from the core. For the pellets with a thicker coating, the remoxipride HCl monohydrate particles which become embedded in the coating are most likely covered by a fresh layer of coating material. Since the Raman measurements were carried out in confocal mode, only the outer part of the coating (around 3 μm) was sampled, hence drug particles embedded more deeply in the coating would not be seen, or would only appear very weakly.

5. Conclusions

The AFM technique has proven to be a powerful tool in the study of dry formulation surfaces as well as in the study of controlled release behavior in liquid cells. The performance of the controlled release preparation in liquid can be conveniently studied by AFM. Especially the changes in the surface coating can be followed during the release process in aqueous solution. This gives further insight into the mechanisms controlling the release of the drug. The dissolution of compounds present at the surface and the change in the surface structure, especially during the first period of release, has been observed. In the present study confocal Raman microimaging has been used to identify the chemical composition in selected small areas of the coating surface confirming the conclusions from the AFM measurements. Although the AFM, SEM, and Raman studies all indicate that polymer-embedded active substance could be an explanation for the release properties for the studied preparation there still are some unclarities. The eventual pore formation starting from depressions and “craters” in the film forming pores, has not been confirmed and is subject to more investigations in an on-going study by combining release studies with SEM with X-ray energy dispersive spectrometry (XEDS). The advantages of AFM in comparison with SEM are several. AFM investigations of polymer coating surfaces can be made with-

out any preparation of the sample and in this respect the method is non-destructive. AFM avoids destroying the surface since it does not involve high-energy beams as in SEM, where the effect of the intense beam on small scanning areas of the metal-coated polymer surface can induce cracks. SEM is not capable of providing information on how the pellet performs in an aqueous environment, which is of major importance when studying pharmaceutical preparations. AFM has a better resolution than SEM. The use of AFM in the future may provide more knowledge about the effects of different procedures used in the manufacturing of pharmaceuticals.

Acknowledgements

Gunnar Zackrisson, AstraZeneca Tablet Production Sweden, is acknowledged for supplying the material. The authors are grateful for the technical assistance in performing SEM measurements given by Helen Hasander.

References

- Borgqvist, P., Zackrisson, G., Nilsson, B., Axelsson, A., 2002. Simulation and parametric study of a film-coated controlled-release pharmaceutical. *J. Control. Release* 80, 229–245.
- Bottomey, L.A., 1998. Scanning probe microscopy. *Anal. Chem.* 70, 425–475.
- Chen, X., Shakesheff, K.M., Davies, M.C., Heller, J., Roberts, C.J., Tendler, S.J.B., Williams, P.M., 1995. Degradation of thin polymer studied by simultaneous *in situ* atomic force microscopy and surface plasmon resonance analysis. *J. Phys. Chem.* 99, 11537–11542.
- Clarke, F.C., Jamieson, M.J., Clarke, D.A., Hammond, S.V., Jee, R.D., Moffat, A.C., 2001. Chemical image fusion. The synergy of FT-NIR and Raman mapping microscopy to enable a more complete visualization of pharmaceutical formulations. *Anal. Chem.* 73, 2213–2220.
- Langer, R., 1993. Polymer-controlled drug delivery systems. *Acc. Chem. Res.* 26, 537–542.
- Lindstedt, B., Ragnarsson, G., Hjärtstam, J., 1989. Osmotic pumping as a release mechanism for membrane coated drug formulations. *Int. J. Pharm.* 56, 261–268.
- Ragnarsson, G., Sandberg, A., Johansson, M.O., Lindstedt, B., Sjögren, J., 1992. In vitro release characteristics of a membrane coated pellet formulation—*influence of drug solubility and particle size*. *Int. J. Pharm.* 79, 223–232.
- Sammon, C., Hajotdoost, S., Eaton, P., Mura, C., Yarwood, J., 1999. Materials analysis using confocal Raman microscopy. *Macromol. Symp.* 141, 247–262.

Sandberg, A., Ragnarsson, G., Jonsson, U.E., Sjögren, J., 1988. Design of a new multiple unit controlled-release formulation of metoprolol—metoprolol CR. *Eur. J. Clin. Pharmacol.* 33, S3–S7.

Shakesheff, K.M., Davies, M.C., Roberts, C.J., Tendler, S.J.B., Williams, P.M., 1996. The role of scanning probe microscopy in drug delivery research. *Crit. Rev.* 13, 225–256.

Shakesheff, K.M., Davies, M.C., Domb, A., Jackson, D.E., Roberts, C.J., Tendler, S.J.B., Williams, P.M., 1994a. In situ atomic force microscopy visualization of the degradation of melt-crystallized poly(sebacic anhydride). *Macromolecules* 28, 1108–1114.

Shakesheff, K.M., Davies, M.C., Roberts, C.J., Tendler, S.J.B., Shard, A.G., Domb, A., 1994b. In situ atomic force microscopy imaging of polymer degradation in an aqueous environment. *Langmuir* 10, 4417–4419.

Shakesheff, K.M., Chen, X., Davies, M.C., Domb, A., Roberts, C.J., Tendler, S.J.B., Williams, P.M., 1995a. Relating the phase morphology of a biodegradable polymer blend to erosion kinetics using simultaneous in situ atomic force microscopy and surface plasmon resonance analysis. *Langmuir* 11, 3921–3927.

Shakesheff, K.M., Davies, M.C., Heller, J., Roberts, C.J., Tendler, S.J.B., Williams, P.M., 1995b. Release of protein from a poly(ortho ester) film during surface erosion studied by in situ atomic force microscopy. *Langmuir* 11, 2547–2553.

Wesselink, J.A., 1993. Controlling diffusion. *J. Control. Release* 24, 47–60.

Zackrisson, G., Oestling, G., Skagerberg, B., Anfaelt, T., 1995. Accelerated dissolution rate analysis (ACDRA) for controlled release drugs. applications to Roxiam. *J. Pharm. Biomed. Anal.* 13, 377–383.